arXiv:1408.5489v1 [cond-mat.mtrl-sci] 23 Aug 2014

Elastic and magnetic properties of cubic Fe_4C from first-principles

Gul Rahman* and Haseen Ullah Jan

Department of Physics, Quaid-i-Azam University, Islamabad 45320, Pakistan

Abstract

First-principles based on density functional theory is used to study the phase stability, elastic, magnetic, and electronic properties of cubic (c)-Fe_4C. Our results show that c-Fe_4C has a ferromagnetic (FM) ground state structure compared with antiferromagnetic (AFM) and nonmagnetic (NM)states. To study the phase stability of c-Fe_4C, BCC Fe_4C, FCC Fe_4C, and BCC $Fe_{16}C$, where C is considered at tetrahedral and octahedral interstitial sites, are also considered. Although, the formation energy of c-Fe_4C is smaller than BCC Fe_4C, but the shear moduli of c-Fe_4C is negative in the FM and AFM states indicating that c-Fe_4C is dynamically not stable in the magnetic (FM/AFM) states. However, NM state has positive shear moduli which illustrates that instability in c-Fe_4C is due to magnetism and can lead to soft phonon modes. The calculated formation energy also shows that c-Fe_4C has higher formation energy compared with the FCC Fe_4C indicating no possibility of c-Fe_4C in low carbon steels at low temperature. The magnetic moment of Fe in c-Fe_4C is also sensitive to lattice deformation. The electronic structure reveals the itinerant nature of electrons responsible for metallic behavior of c-Fe_4C.

I. INTRODUCTION

The mechanical properties of steels can be improved by various types of solute atom, which helps to pin the dislocations. The base ingredient of steel is Fe, depending on the temperature, adopts different crystal structures. For example, at 912 K, α-Fe, *i.e.*, body centred cubic (BCC) transforms to γ-Fe face centred cubic (FCC), which further transforms to δ-Fe at 1700 K. Light elements, like H, C, and N are considered to be playing a significant role in the phase stability and mechanical strength of Fe. Compared to the host Fe atom, radii of light atoms are smaller so they do not substitute them and prefer to sit at the the interstitials sites.[1] However, recent reports show that at the surfaces of both α-Fe and γ-Fe, C at the substitutional sites significantly reduces the surface energy[2,3] so it prefers substitutional over the interstitials.

Iron carbides are of crucial importance in the design of the mechanical properties of steels and other iron alloys.[4–8] Carbon interstitials are also present in various iron carbide phases (Fe_2C, Fe_3C, Fe_7C_3, $Fe_{16}C$) as precipitates in a ferrite matrix or in pearlite-type or banite-type microstructures[4–7]. Experimental investigations[9,10] of martensites have indicated that the octahedral interstitial sites are preferred locations for carbon atoms in the BCC iron structure. The tetragonal distortion of the martensitic lattice is generally regarded as direct evidence of an unequal distribution of carbon atoms over the three available octahedral interstitial sublattices. When the carbon atoms occupy a single sub-lattice within an otherwise BCC iron lattice, the microscopic lattice symmetry is reduced to tetragonal, and a tetragonal distortion of the BCC iron lattice results. Zener[11] treated the thermodynamics of such carbon ordering, and the tetragonal martensite is accordingly referred to as "Zener-ordered." It was shown[12–14,16] that a secondary ordering of carbon interstitials may occur within the Zener sublattice during martensite aging, prior to the detection of ϵ- or ϵ'-carbide. These results have been interpreted in terms of the formation of the Fe_4C phase with a considerable deviation from stoichiometric composition.[14]

In the past much attention has been focused to interstitial C in BCC Fe, *i.e.*, Fe_4C and FCC Fe, *i.e.*, Fe_4C.[17] There is an other possible phase of Fe-C system—cubic Fe_4C denoted as c-Fe_4C (see Fig.1). In this phase, the C atoms are not located at interstitial sites, but at the regular lattice sites. There are four Fe atoms and one C atom per unit cell and has a lattice constant of 3.89 Å.[15] This structure has a pearson symbol "cP5" and belongs

to the space group "P43m". The fractional atomic positions of Fe and C atoms are given in Table I. Due to its very different crystal structure than those of other iron carbides, it is very important to investigate its physical properties from first-principles and to see any possibility of formation in steels, because there is no theoretical work has been done on c-Fe_4C. We study the phase stability, elastic, magnetic, and electronic properties of c-Fe_4C. Three different magnetic states, *i.e.*, non-magnetic (NM), ferromagnetic (FM), and anti-ferromagnetic (AFM) states (see Fig.1) of the c-Fe_4C are considered. To compare the structural properties of c-Fe_4C, we also considered BCC Fe_4C, $Fe_{16}C$ and FCC Fe_4C. These results will be helpful for understanding the relative stability of iron and iron carbides in steels.

II. CALCULATION METHODS

A. Computational Details

All calculations were carried out using the SIESTA[18] *ab initio* density functional theory[19] code. We used the spin-polarized Perdew-Burke-Ernzerhof (PBE) version[20] of the Generalised Gradient Approximation (GGA) to the exchange and correlation functional. Using Troullier-Martins parametrization[21] and one projector for each l state, core electrons are described by norm-conserving pseudopotentials. We used double-ζ polarized (DZP) basis sets optimised for solid Fe and C. Different meshes were used for the real space discretization. Finally, a mesh cut off of 400 Ry for real space discretisation and an $m \times m \times m$ ($m = 8$) Monkhorst-Pack grid[18] for Brillouin zone (BZ) sampling were used. The latter corresponds to k points in the irreducible part of the BZ. Both lattice parameters and coordinates of atoms were optimized.

B. Method for formation energies

The formation energy (ΔE) of an iron carbide Fe_nC_m is described as,

$$\Delta E = E(\mathrm{Fe_nC_m}) - [\mathrm{nE(Fe)} + \mathrm{mE(C)}] \quad (1)$$

In the above equation $E(\mathrm{Fe_nC_m})$ is the total energy of FeC systems. Similarly E(Fe) and E(C) represent the total energy of elemental solids, where n and m are number of Fe and C

atoms, respectively. We considered both the α and γ phases of Fe, and diamond C for the evaluation of the formation energy. The relative stability of c-Fe_4C with respect to various iron carbides is determined by the formation energy per atom, given by

$$\Delta E_f = \Delta E/(\mathrm{n} + \mathrm{m}) \tag{2}$$

Here, negative values of ΔE_f means that Fe_nC_m is more stable than the parent solids.

C. Method for Elastic Properties

Elastic properties can better be understood by calculating elastic constants C_{ij}. For this, volume conserved strain matrices[22] are applied to deform the lattice. A ± 0.03 amount of strain (ε) is imposed on the cubic (c), BCC, and FCC phases of Fe_4C, where different magnetic states, *i.e.*, NM, FM and AFM are considered. The total energies were calculated as a function of lattice volume and fitted to the Birch-Murnaghan equation of state (EOS),[23] to find the optimized lattice volumes and the bulk moduli. Cubic systems are well described by three independent elastic constants, *i.e.,* C_{11}, C_{12}, and C_{44}, where these elastic constants represents deformations along different diagonals in a unit cube of the lattice. The three elastic constants are determined by calculating the total energy as a function of the bulk volumetric shears.[22]

III. RESULTS AND DISCUSSIONS

A. Formation energies and phase stabilities

Formation energy is a measure of the phase stability of a system. Before calculating the formation enthalpy, we first optimized the lattice parameters for the α and γ phases of Fe, diamond C, and Fe_4C in different phases, *i.e.*, cubic , BCC, and FCC in different magnetic states, *i.e.*, NM, FM, and AFM.

Our optimized lattice parameters are presented in Table II. We see that our calculated lattice parameters of Fe and C are in good agreement with the previous theoretical and experimental work.[17,24,25] The c-Fe_4C expands by about 2.63% in both the magnetic phases as compared to the non-magnetic phase. This magneto-volume effect has significant influence

on the elastic and magnetic properties as discussed shortly. The representative binding energy curves of NM, FM, and AFM states for the c-Fe_4C are shown in Fig.2. It is clear from this figure that FM has the lowest energy with lattice constant 3.89 Å. Therefore our DFT calculations show that FM is the magnetic ground state. The calculated lattice constants for the BCC and FCC Fe_4C are 2.93 Å and 3.82 Å , respectively, in the FM ground states. Previous results for the FCC Fe_4C are 3.76 Å [17] and 3.87 Å [26] in theory and experiment,the present calculated values are slightly smaller than those obtained at room temperature, as might be expected from thermal expansion, but it is encouraging that the trend of the lattice parameter as compared with elemental solids (Fe, C) are correctly reproduced (see Table II).

Manipulating the optimized lattice parameters, formation energy is calculated using Eq.(1) and the results are tabulated in Table III. Formation enthalpy is nothing more than the total energy of a system at zero pressure and zero kelvin at the corresponding equilibrium lattice constant. The formation enthalpy is measured relative to BCC Fe, FCC Fe, and diamond C for all the Fe-C systems. For the purpose of phase stability, we also considered BCC Fe_4C and $Fe_{16}C$, where C atom is considered at octahedral and tetrahedral positions. BCC Fe_4C and $Fe_{16}C$ were model as $1\times 1\times 2$ and $2\times 2\times 2$ supercells, respectively, and the C atom was considered at octahedral and tetrahedral sites. Our calculated formation enthalpy for the $Fe_{16}C$ at the octahedral and tetrahedral sites with respect to the BCC Fe lattice are 32.057 and 32.062 kJ/mol, respectively (see Table III), which are in good agreement with the previous work, *i.e.*, 20.19 kJ/mol at the octahedral and 24.89 kJ/mol at the tetrahedral site,[27] also ΔE_f for the BCC Fe_4C is 116.363kJ/mol at the octahedral, and 100.830 kJ/mol at the tetrahedral lattice sites. The formation enthalpy at both the octahedral and tetrahedral Fe_4C is larger than $Fe_{16}C$ due high carbon concentration. Table III clearly shows that FCC Fe_4C has the lowest formation energy, *i.e.*, -3.751 kJ/mol with respect to the FCC Fe lattice and highest one, *i.e.*, 89.899 kJ/mol with respect to the BCC Fe lattice. It shows that FCC Fe_4C with respect to the FCC Fe lattice is the most stable phase among these Fe-C systems. This is also in agreement with the experimental observations.[24] In all these interstitial carbides, we see that Fe_nC_m has the lowest formation enthalpy with respect to BCC Fe lattice. It is noticeable that c-Fe_4C has lower formation energy than BCC Fe_4C with respect to both, *i.e.*, BCC and FCC Fe lattices, however this is dynamically not a stable structure which will be discussed below. This indicate, that it will not be easy for C to form such c-Fe_4C structure in low carbon steels.

B. Elastic properties

In order to obtain the elastic properties, we followed our previous approach[22] and ± 0.03 amount of strains was imposed, using the shear and elastic volume conserved deformation matrices. The calculated bulk moduli and elastic constants are given in Table IV. The calculated elastic constants of BCC Fe and diamond C are close to the experimental values[25] and confirm that the number of basis functions and the number of k-points used in these calculations are sufficient to reproduce the experimental data for Fe and C. It is noticeable that BCC Fe and diamond C have positive shear modulus, whereas FCC Fe has negative one which indicates that FCC Fe is dynamically unstable and BCC Fe is the most stable structure of Fe. Also note that the FCC Fe_4C has positive elastic constants, which further demonstrate the phase stability of C interstitials in FCC Fe. This is also very encouraging that C free FCC Fe is not stable, however it becomes stable when C is placed at the octahedral interstitial site. This phase stability is accompanied by the volume expansion (see Table V), and reduction of magnetization which will be discussed below. We may also infer from these calculations that the FCC Fe either can be stabilized in the form of a thin film on a substrate, *e.g.*, Cu or by inserting C at the interstitial sites.[29] Moreover, the formation energy of FCC Fe_4C with respect to BCC Fe is found to be 89.899 kj/mol which further illustrates the formation of FCC Fe_4C over BCC Fe_4C.

To discuss the elastic properties of c-Fe_4C, we calculate elastic constants C_{ij} in the NM, FM, and AFM states. The representative curves of C_{ij} in the FM state are shown in Fig.3. In the magnetic (FM/AFM) states c-Fe_4C has negative curvature, but not in the NM case (see Table IV). This shows that c-Fe_4C is dynamically not stable due to magnetism. In other words, c-Fe_4C may be stable at a very high temperature due to thermal expansion and the high temperature will destroy the magnetic state of c-Fe_4C as well. To further explore the elastic properties of c-Fe_4C, we also calculated C_{ij} at different lattice constants, *i.e.*, 3.89Å — 3.85Å (volumes) in the FM state and the results are summarized in Table V. It is clear to see that the absolute values of C_{12} and C_{44} increase, where as and C' and C_{11} decrease with decreasing volume. Note that C' remains negative in the whole volume (lattice) range. This clearly indicates that the phase instability is coming from the magnetic interactions of C atom with the nearest Fe atoms. This shows that magnetization mainly helps to stabilize and destabilize ferrous materials.[22,30]

C. Magnetism

We calculated the magnetic moment per Fe atom for the BCC and FCC Fe, Fe_4C and the results are summarized in Table VI. Our calculated values agree with the the available experimental work. The magnetic moments of pure BCC and FCC Fe are $2.24\,\mu_B$ and $3.59\,\mu_B$, respectively and are in good agreement with experiments $2.22\,\mu_B$ (BCC Fe)[25] and theory $3.36\,\mu_B$ (FCC Fe).[26] In c-Fe_4C each Fe atom contributes approximately equal magnetic moment ($2.11\,\mu_B$) due to the same lattice symmetry. On the other hand BCC Fe_4C has $1.77\,\mu_B$ per Fe atom, where FCC Fe_4C has $2.04\,\mu_B$ per Fe atom. The previous theoretically calculated magnetic moment for the FCC Fe_4C is $2.98\,\mu_B$ per Fe atom.[26] We see that the magnetic moments are slightly decreased in Fe_nC_m. We also considered the effect of lattice volume on the magnetic moments of c-Fe_4C, which are presented in Fig.4. This figure shows that magnetic moment increases with lattice volume as found in the other Fe-based systems.[28] This increment is mainly due to weak hybridization effect at higher volume. We can see an abrupt change in the magnetic moments around 3.85—3.90 Å. This abrupt change in magnetic moment indicates that c-Fe_4C is very sensitive to lattice deformation which can be lead to the phase stability of the system. This abrupt change may be due to spin-flip effect.[28]

In de-localized electron systems, magnetism originates from the difference in the spin up and spin down bands' populations. Also deformation affects de-localized systems drastically due to strong interaction of magnetic moments and it would be very necessary to study the effects of deformation. As shown above that c-Fe_4C is dynamically not stable in the FM/AFM state. To further investigate the effect of strain on magnetism, we applied ± 0.07 volume conserved strains for different lattice constants, which was varied from 3.89 Å to 3.85 Å. The results are summarized in Fig.5. The magnetic moment decreases with decreasing lattice volumes consistent with Fig. 4, *i.e.*, magnetic moment is maximum at the optimized lattice constant (3.89 Å) and decreases up to (3.85 Å). At each lattice constant, the magnetic moment of the un-strained system is maximum and decreases as the strain increases. The magnetism of c-Fe_4C is very sensitive around $c/a = 1.0$, and at large elongation the magnetic moments of c-Fe_4C are saturated, whereas at large compressions the magnetic moment decreases. Also, the maximum in the magnetic moment shifts to smaller value of c/a at smaller volume of c-Fe_4C. Such magnetic behaviour clearly indicates that

c-Fe_4C is dynamically unstable due to magnetism.

D. Electronic structure

Elastic and magnetic properties and phase stability and instability ultimately have an electronic origin. Fig.6 represents the total and atomic projected density of states (PDOS) in the FM state of c-Fe_4C. The total DOS of c-Fe_4C has low lying sharp peaks coming from the hybridization of C and Fe atoms. The DOS of c-Fe_4C shows that the t_{2g} and e_g states of Fe-d are almost degenerate which is quite different from BCC/FCC Fe and BCC/FCC Fe_4C. Near the Fermi energy, C and Fe atoms also hybridises and the DOS shows metallic behavior. The metallicity of c-Fe_4C consistent with the pure α and γ-Fe. The strong bonding nature of Fe-C in c-Fe_4C is also visible in charge density plot which is shown in Fig.7. This strong bonding is responsible for the smaller magnetic moments of Fe in c-Fe_4C as compared with the BCC/FCC Fe.

IV. SUMMARY

The elastic and magnetic properties of c-Fe_4C are studied using first-principles calculations. Different magnetic phases (NM, FM, and AFM) of c-Fe_4C were considered, and we found FM ground state for c-Fe_4C. For the phase stability of c-Fe_4C, BCC Fe_4C, FCC Fe_4C, and BCC $Fe_{16}C$, where C was located at tetrahedral and octahedral interstitial sites, were also considered. The formation energy of c-Fe_4C was smaller than BCC Fe_4C, but the shear moduli of c-Fe_4C was negative in the FM and AFM states indicating that c-Fe_4C is dynamically not stable in the magnetic (FM/AFM) states. In contrast, NM state showed positive shear moduli which illustrates that instability in c-Fe_4C is due to magnetism. The magnetic moment of c-Fe_4C increases with increasing lattice constant, similar to BCC Fe. The effect of lattice distortion on magnetic moments with different lattice constants were also studied and it was confirmed that magnetic moments decreases with strain. We concluded that c-Fe_4C can not form a stable phase in low carbon steels at low temperature. The electronic density of states and charge density revealed metallic behavior of electrons in c-Fe_4C.

ACKNOWLEDGMENT

G. R. acknowledges the cluster facilities of NCP, Pakistan.

---

* gulrahman@qau.edu.pk

[1] H. K. D. H. Bhadeshia and Sir Robert Honeycombe, Steels Microstructure and Properties, *Third edition.*

[2] E. J. Song, H. K. D. H. Bhadeshia, and D. W. Suh, Corrosion Science, **77**, 379, (2013).

[3] S. S. Baik, B. I. Min, S. K. Kwon, and Y. M. Koo, Phys. Rev. B **81**, 144101 (2010).

[4] L. J. Hofer and E. M. Cohen, Nature. **167**, 977 (1951).

[5] D. H. Jack and K. H. Jack, Mater. Sci. Engin. **11**, 1 (1973).

[6] H. J. Goldschmidt and J.Iron Steel Inst. **160A**. 345 (1948).

[7] S. Nagakura and S. Oketani, Transactions. **ISIJ 8**, 265 (1968).

[8] M. Taneike, F.abe, and K. Sawada, Nature. **424**, 294 (2003).

[9] I. R. Entin, V. A. Somenkov, and S. Sh. Shil'shtein, Sov. Phys. Dokl. **17**, 1021 (1973).

[10] R. Kaplow, M. Ron, and N. Decristofaro, Metall. Trans. A **14A**, 1135 (1983).

[11] C. Zener, Trans. AIME **167**, 550 (1946).

[12] W. K. Choo and R. Kaplow, Acta Metall. **21**, 725 (1973).

[13] V. I. Izotov and L. M. Utevskiy, Phys. Met. Metallogr. **25**, 86 (1968).

[14] H. Ino, T. Ito, S. Nasu, and U. Gonser, Acta Metall. **30**, 9 (1982).

[15] http://cst-www.nrl.navy.mil/lattice/struk/Fe4C.html

[16] S. Nagakura and M. Toyoshima, Trans. JIM **20**, 100 (1979).

[17] Nicolas *et. al.*, Phys. Rev. B **71**, 205214 (2005).

[18] P. Ordejon, E. Artacho, and J. M. Soler, Phys. Rev. B **53**,10441 (1996);

[19] W. Kohn and L. J. Sham Phys. Rev. Vol. 140 (1965)

[20] J. P. Perdew, K. Burke, and M. Ernzerhof Phys. Rev. Lett. **77**, 3865 (1996)

[21] Troullier N and Martins J 1991 Phys. Rev. B **43**, 1993-2006

[22] G. Rahman, I. G. Kim, and H. K. D. H. Bhadeshia, J. Appl. Phys. **111**, 063503 (2012)

[23] F.Birch, Phys.Rev. **71**, 809 (1947); F. D. Murnaghan, Proc. Natl. Acad. Sci. U.S.A. **30**, 244 (1944).

[24] C. M. Fange *et. al.*, Phys. Rev. B **85**, 054116 (2012).

[25] *Introduction to solid state physics* 8th Edition

[26] K. Oda, H. Fujimura,H. Ino, J. Phys.: Condens. Matter **6**, (1994).

[27] J. H. Jang *et. al.*, Scripta Materialia **68**, 195-198 (2013).

[28] A. V. dos Santos *et. al.*, Journal of Magnetism and Magnetic Materials **166**, (1997).

[29] A. Kirilyukm *et. al.*, Phys. Rev. B **54**, 2 (1996).

[30] O. I. Gorbatov *et. al.*, The Physics of Metals and Metallography **114**, 8 (2013).

TABLE I. Atomic fractional coordinates of c-Fe_4C structure.

Atom	x	y	z
Fe	0.265	0.265	0.265
Fe	0.265	-0.265	-0.265
Fe	-0.265	0.265	-0.265
Fe	-0.265	-0.265	0.265
C	0.0	0.0	0.0

TABLE II. Calculated lattice constants for BCC and FCC Fe, diamond C, and Fe_4C in different magnetic states and crystal structures. The lattice constants for NM, FM, and AFM states are given in units of Å.

System	This Work		Experiment
BCC (Fe)	2.86	2.86[a]	2.83[b]
FCC (Fe)	3.68	3.58[b]	3.60$_b$
Diamond (C)	3.56	3.56[a]	3.57[c]
c-Fe_4C(NM)	3.79	- -	
c-Fe_4C(FM)	3.89	- -	
c-Fe_4C(AFM)	3.89	- - -	
BCC (Fe_4C)	2.93	- -	
FCC (Fe_4C)	3.82	3.87[d]	3.76[c]

a Ref.[25]

b Ref.[24]

c Ref.[17]

d Ref.[26]

TABLE III. Calculated formation enthalpies per atoms (ΔE_f) in units of (kJ/mol) with respect to BCC and FCC Fe for different phases of Fe_4C. TET and OCT stand for tetrahedral and octahedral interstitial sites.

System	BCC ΔE_f	FCC ΔE_f
TET Fe_4C	100.830	113.463
TET $Fe_{16}C$	32.062	85.961
OCT Fe_4C	116.363	132.878
OCT $Fe_{16}C$	32.057	85.940
c-Fe_4C	46.339	45.348
FCC Fe_4C	89.899	-3.751

TABLE IV. Calculated Elastic constants and bulk modulii in units of Giga Pascal (GPa) for different systems.

System Name	C_{11}	C_{12}	C_{44}	B	$\acute{C}$
BCC Fe	257.436	137.216	100.184	177.290	60.11
FCC Fe	67.762	189.430	-46.610	148.874	-60.83
Diamond C	1091.420	182.612	571.482	485.548	454.40
c-Fe_4C (FM)	-	-	80.300	174.965	-4.07
c-Fe_4C (NM)	252.141	195.864	147.733	214.623	28.13
FCC-Fe_4C	400.204	164.088	25.490	242.793	118.05

TABLE V. The calculated elastic constants (GPa) and shear modulus $\acute{C}$ for c-Fe_4C, obtained at different lattice constants.

a (Å)	C_{11}	C_{12}	C_{44}	$\acute{C}$
3.89	146.15	189.38	80.30	-21.61
3.88	145.5	189.7	80.00	-22.09
3.87	143.44	190.57	81.03	-23.39
3.86	141.72	191.6	83.85	-24.93
3.85	140.62	192.15	82.85	-25.76

TABLE VI. The DFT calculated total magnetic moment per Fe atom (μ_B) for the BCC and FCC Fe, and different crystal structures of Fe_4C in units of the Bohr magneton (μ_B) are well compared with the available literature (theory and experiment). LS and HS in the subscripts stand for low spin and high spin, respectively.

System Name	This Work	Experiment	Theory
BCC (Fe)	2.24	2.22[a]	2.15[b]
FCC (Fe)	3.59	-	0.126^{c}_{LS}, 3.359^{c}_{HS}
c-Fe_4C	2.11	-	-
BCC Fe_4C	1.77	-	-
FCC Fe_4C	2.04	-	2.98[c]

a Ref.[25]

b Ref.[24]

c Ref.[26]

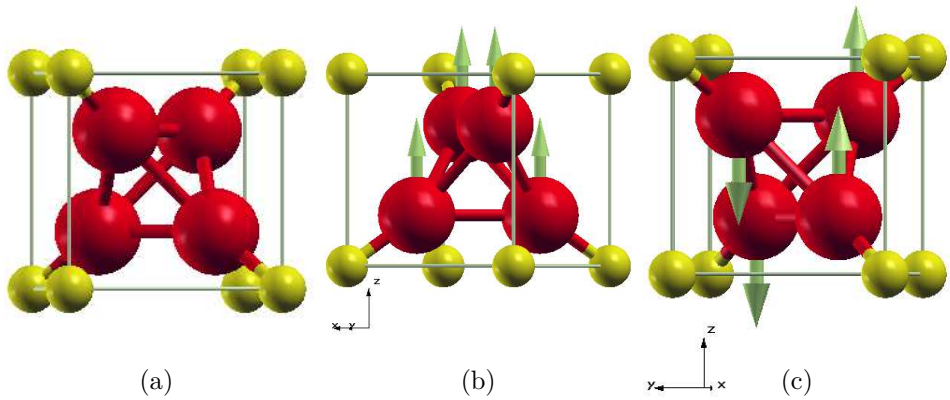

FIG. 1. (Colour online) Crystal structures of c-Fe_4C in the NM (a), FM (b), and AFM (c) states. The up and down arrows show the direction of spin magnetic moments. Red (yellow) balls show Fe (C) atoms.

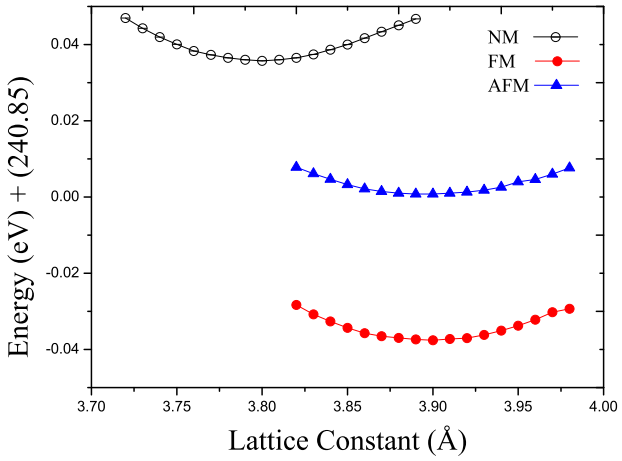

FIG. 2. (Colour online) Calculated total energy vs lattice constant in different magnetic states of c-Fe_4C. The empty circles, filled circles, and filled triangles represent the NM, FM, and AFM states of c-Fe_4C, respectively.

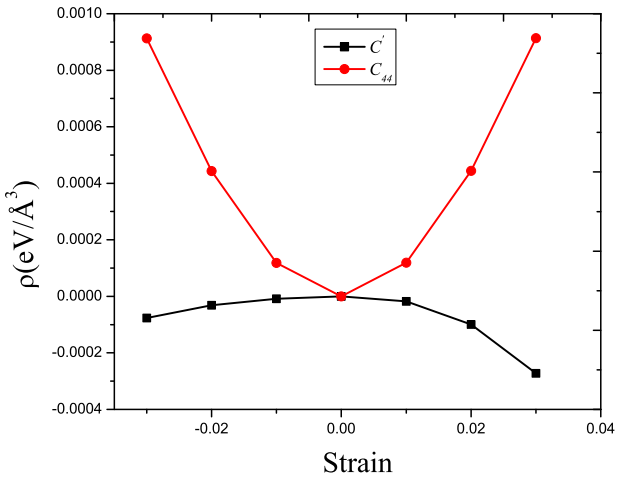

FIG. 3. (Colour online) Calculated energy density (ρ) vs strain for the shear modulus $\acute{C}$ (black filled squares) and elastic constant C_{44} (red filled circles) of c-Fe_4C in the FM state.

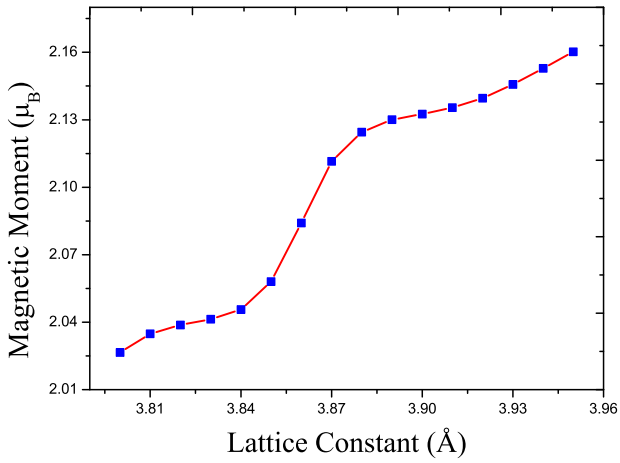

FIG. 4. (Colour online) The calculated total magnetic moment (μ_B) per Fe atom vs lattice constant (Å) of c-Fe_4C.

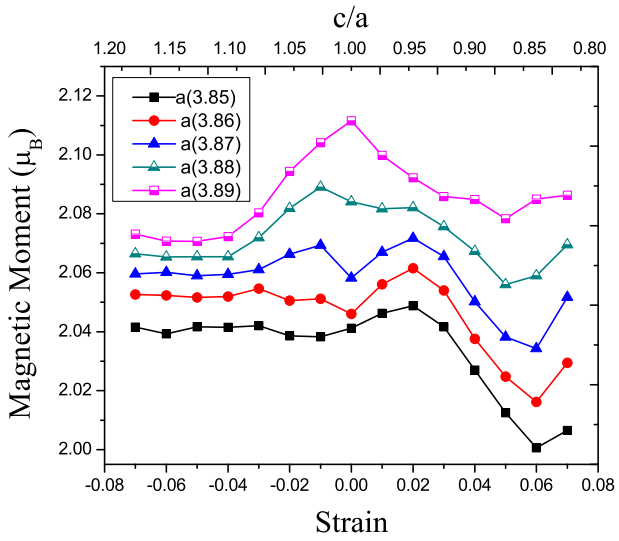

FIG. 5. (Colour online) Strain(c/a) vs calculated magnetic moment (μ_B) per Fe atom of c-Fe_4C. Filled squares (black), filled circles (red), filled triangles (blue), half filled triangles (misson), and half filled squares (magenta) represent lattice constants from 3.85—3.89Å of c-Fe_4C.

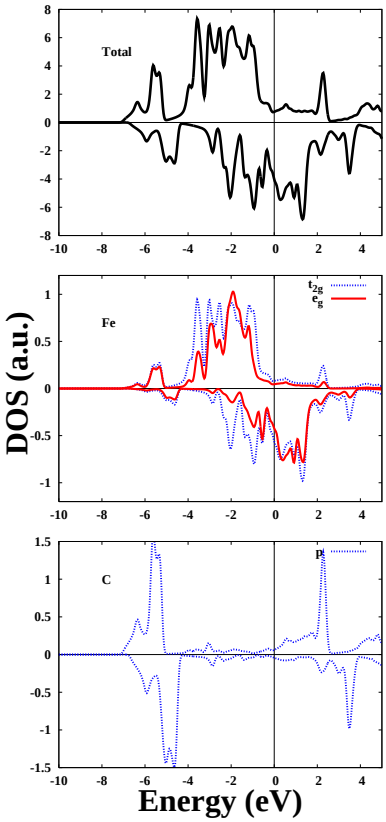

FIG. 6. (Colour online) Calculated total density of states (DOS) for c-Fe_4C in FM state, and partial density of states (PDOS) of Fe and C atoms. Solid (red) and dashed (blue) lines represent e_g and t_{2g} states of Fe. Bottom panel of blue dotted lines represent C p states. Top panel solid line represents total DOS. The positive (negative) DOS shows majority (minority) spin states. The Fermi level (E_F) is set to zero.

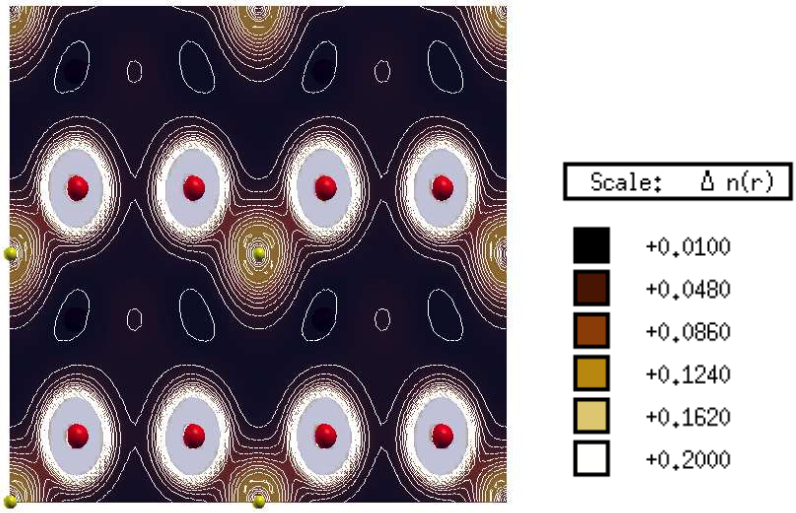

FIG. 7. (Colour online) Charge density contour along the (110) plane of the c-Fe_4C. Red and yellow balls represent Fe and C atoms, respectively. The cut-off plane is passing through the second neighbour atoms. Darker and lighter regions corresponds to low and high charge density. The scale is also shown.